Aging Brain 5 (2024) 100119

Contents lists available at ScienceDirect

Aging Brain

journal homepage: www.elsevier.com/locate/nbas

Microbiome-driven alterations in metabolic pathways and impaired cognition in aged female TgF344-AD rats

Abbi R. Hernandez [a,*], Erik Parker [b], Maham Babar [a], Anisha Banerjee [a], Sarah Ding [a], Alexis Simley [a], Thomas W. Buford [a,c]

[a] Department of Medicine, Division of Geriatrics, Gerontology & Palliative Care, University of Alabama at Birmingham, Birmingham, AL 35205, USA
[b] Department of Epidemiology and Biostatistics, School of Public Health, Indiana University-Bloomington, Bloomington, IN 47405, USA
[c] Birmingham/Atlanta VA GRECC, Birmingham VA Medical Center, Birmingham, AL 35244, USA

ARTICLE INFO

Keywords:
Alzheimer's
Microbiome
Aging
Cognitive decline
Metabolism

ABSTRACT

Alzheimer's disease (AD) not only affects cognition and neuropathology, but several other facets capable of negatively impacting quality of life and potentially driving impairments, including altered gut microbiome (GMB) composition and metabolism. Aged (20 + mo) female TgF344-AD and wildtype rats were cognitively characterized on several tasks incorporating several cognitive domains, including task acquisition, object recognition memory, anxiety-like behaviors, and spatial navigation. Additionally, metabolic phenotyping, GMB sequencing throughout the intestinal tract (duodenum, jejunum, ileum, colon, and feces), neuropathological burden assessment and marker gene functional abundance predictions (PICRUSt2) were conducted. TgF344-AD rats demonstrated significant cognitive impairment in multiple domains, as well as regionally specific GMB dysbiosis. Relationships between peripheral factors were investigated using Canonical Correspondence Analysis (CCA), revealing correlations between GMB changes and both cognitive and metabolic factors. Moreover, communities of gut microbes contributing to essential metabolic pathways were significantly altered in TgF344-AD rats. These data indicate dysbiosis may affect cognitive outcomes in AD through alterations in metabolism-related enzymatic pathways that are necessary for proper brain function. Moreover, these changes were mostly observed in intestinal segments required for carbohydrate digestion, not fecal samples. These data support the targeting of intestinal and microbiome health for the treatment of AD.

Background

Currently, nearly 6 million Americans are living with Alzheimer's disease (AD), placing significant emotional and financial burden on themselves and their caregivers [1]. Translation of interventions targeting AD have been largely unsuccessful thus far, demonstrating great need for alternative strategies. Not only does AD impact cognitive function, but it also increases risk of metabolic impairment by 65 % [2] and may lead to gut dysbiosis (i.e., disrupted microbiota composition and/or diversity) [3,4]. Gut health and microbiome (MB) composition play a large role in energy homeostasis and metabolic function, which in turn greatly influence cognitive performance [5–7]. Therefore, one potential avenue through which the gut may exert control over neurobiological health along the gut-brain-axis [8,9] is through regulation of systemic metabolism, which itself strongly influences both of these organ

* Corresponding author.
E-mail address: Abigailhernandez@uabmc.edu (A.R. Hernandez).

https://doi.org/10.1016/j.nbas.2024.100119
Received 15 January 2024; Received in revised form 9 May 2024; Accepted 28 May 2024

systems [10,11]. Consequently, gut-derived impairments in peripheral and brain metabolic functioning may underlie cognitive impairments associated with AD. Thus, we investigated cognitive and peripheral health status in an aged TgF344-AD rat model of AD [12].

Significant pathology and altered cognitive status have been reported in these rats [12–15], and more recently some indicators of metabolic health [16], an aspect of AD often missed in other transgenic models. Herein we expand upon these data by investigating cognitive status, metabolic health, physical composition and gut microbiome composition in aged TgF344-AD rats. Though there is evidence of impaired reversal learning [13], fear memory extinction in males [15], and spatial navigation [17], there is a dearth of information regarding higher order tasks requiring the integration of information across several brain structures in these transgenic rats. Long-range projection neurons that support such complicated cognitive loads are not only the most energetically costly neurons in the brain, but are significantly impacted by age [18] and AD [19]. Therefore, we characterized the effects of AD and age on a working memory/biconditional association task. This task is known to be vulnerable to aging and more sensitive than single-modality tasks like the Morris water maze [20–23].

There are several avenues through which gut function and health influences cognition within or outside of the context of AD, which may be the result of gut dysbiosis. This includes altered production and utilization of neurotransmitters and metabolites (such as short chain fatty acids (SCFA)), or through changes in intestinal permeability. Only female subjects were utilized, as markers of glucose metabolism and body composition differences were previously observed in females, but not males [16]. Moreover, due to the extreme long-standing bias of the field towards the utilization of male subjects in medical research, there is much less known about the influence of AD-related peripheral health factors in females, despite the higher prevalence of AD in females than males [24–26]. Interestingly, individuals with AD have disrupted preference and intake of carbohydrates [27]. Carbohydrates are digested within the small intestine (along with most nutrients) [11,28], yet fecal microbiome populations largely represent colonic GMB populations [29]. Therefore, it is imperative to not only investigate how the microbiome changes in distal large intestine, but portions of the small intestine as well, as we hypothesized that alterations in the GMB differ along the length of the intestinal tract. Gut microbiome alterations with in the TgF344-AD rat model have, to our knowledge, never been characterized in any female subjects of advanced age nor has the intestinal microbiome been described in a regionally-specific manner at any age or sex, though differences in middle and advanced age male rats have been published [30]. Additionally, there are sex-specific effects in other transgenic rodent models of AD, with transgenic AD mice displaying a greater disparity across sex than their wildtype counterparts [31]. Herein, we expand upon these previous works by not only including females, but also by including analyses predicting the functional relevance of gut microbiome alterations for the first time in this rat model, and relate this to cognitive and metabolic decline in AD.

Methods

Subjects and handling

Rats for this study were bred in-house utilizing a descendent from a breeding pair that was originally obtained from University of Southern California [12] and wildtype dams from Envigo RMS LLC (Indianapolis, IN, USA). Heterozygotes harbor the human Swedish mutation amyloid precursor protein (APP^{swe}) and the presenilin-1 exon 9 deletion mutant ($PS1^{\Delta E9}$) and express both tau and amyloid

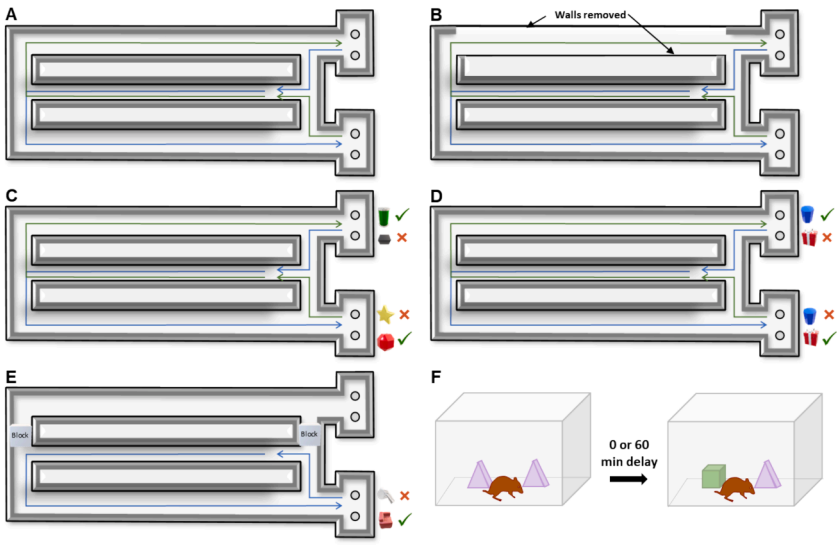

Fig. 1. Behavioral testing apparatus utilized for (A) continuous spatial alternations, (B) open arm assessment of anxiety-like phenotype on continuous spatial alternation ability, (C) working memory object discrimination (WMOD), (D) working memory biconditional association task (WMBAT), (E) simple object discrimination (SOD) and (F) novel object recognition tasks.

pathology [12]. Genotype was confirmed at weaning and again postmortem by Transnetyx using real-time PCR.

Nine wildtype (WT) and 10 Transgenic-AD (TgAD) rats (average starting age = 16.7 months) were initially included in the study. However, only 5 rats of each genotype survived until the end of the study (average age of rats that survived to the end of the study = 25.1 months at study conclusion, range = 24.9–25.8 months), and thus only these 10 rats were included in all analyses unless stated otherwise. Each rat was housed individually and maintained on a 12-hr light/dark cycle with behavioral experiments performed exclusively during the light phase of the cycle due to limitations in housing availability during COVID restrictions. All rats were restricted to approximately 80–85 % of their free feeding body weight to encourage appetitive motivation in behavioral assays. While on food deprivation, rats were weighed a minimum of 3 times weekly. All breeding and experimental procedures were performed in accordance with National Institutes of Health guidelines and were approved by Institutional Animal Care and Use Committees at the University of Alabama at Birmingham.

Behavioral analysis

Testing apparatus and habituation

All behavioral analysis, excluding novel object recognition and elevated plus maze, were conducted on a continuous alternation maze (CAM) with object choice platforms (Fig. 1). This maze allows for simultaneous assessment of spatial navigation and awareness with object recognition and multimodal association tasks [21–23,32]. Rats were habituated to the maze for 10 min per day for 2 consecutive days, during which froot loops (Kellogg Company, Battle Creek, MI) were scattered throughout the maze and rats were encouraged to explore the entirety of the maze.

Spatial alternation and anxiety-like behavioral assessments

Following maze habituation, rats were trained to alternate between the left and right arms of the maze (Fig. 1A). Correct turns were rewarded with a froot loop placed randomly in one of the wells within the correct arm. Incorrect turns were not rewarded. Rats were trained on this task until they were alternating correctly $\geq$ 80 % of the time on 2 consecutive days.

Following this criterion alternation performance, an anxiety-like phenotype was then measured in two ways. Firstly, the walls were removed from one arm of the maze (counterbalanced across rats) and rats were returned to the alternation task (Fig. 1B). Correctly alternating continued to result in a froot loop reward, thus rats were incentivized to equally traverse the open 'risky' arm and the closed 'safe' arm. Secondly, rats were placed in the center of an elevated plus maze (EPM) and allowed to freely ambulate throughout the apparatus for 5 min. Activity was recorded with an overhead camera using the tracking system Ethovision XT (Noldus Information Technology Inc., Wageningen, the Netherlands).

Object discrimination-based behavioral assessment

Once rats were again alternating correctly $\geq$ 80 % of the time on 2 consecutive days, rats progressed to a series of tasks requiring object discriminations of varying difficulty [21,22] with persistent alternation throughout the maze. The Working Memory Object Discrimination (WMOD) task was administered for 3 days. For this task, rats were presented with a unique pair of objects within each arm (i.e. objects A and B in left arm, objects C & D in right arm). One object was always correct within each arm, regardless of which well they were positioned over (Fig. 1C). Rats were trained on this task until they achieved $\geq$ 80 % on 2 consecutive days. The number of incorrect trials required to reach criterion performance was recorded as a measure of learning ability.

Once criterion performance was achieved on the WMOD task, rats progressed to the Working Memory/Biconditional Association task (WMBAT). This task required not only spatial alternation, spatial awareness and object recognition, but the integration of each of these modalities (Fig. 1D). Rats were trained until they achieved $\geq$ 80 % correct (with a minimum of 75 % within each individual arm on at least one of those days) on 2 consecutive days or for a maximum of 60 days of testing. The number of incorrect trials required to reach criterion performance, or maximum trial allowance, was recorded as a measure of learning ability. Specifically, these data demonstrate the rats' ability to form and recall associative memories.

Finally, a simple object discrimination task (SOD) was conducted to investigate the potential for physical impairments in rats' ability to perform the tasks. To do so, one arm was blocked off and rats were rehabituated to the maze for one day (Fig. 1E). During testing, rats ambulated throughout the maze in a continuous loop with an object choice on each trial, during which rats were presented with two objects, with one of the objects always rewarded regardless of where it was presented.

Novel object recognition task

To investigate a simple measure of object recognition memory, a novel object recognition (NOR) paradigm was conducted. Rats were first habituated to a 51 cm $\times$ 36 cm $\times$ 32 cm arena for 10 min per day for two days immediately prior to testing. Additionally, rats were habituated to the testing room for 30 min each day prior to habituation and testing. Lighting conditions were kept low and a white noise machine was utilized for the duration. Rats were tested on the novel object recognition task twice on two consecutive days. One session had no delay between the sample and test phase and the other session had a one-hour delay (counterbalanced across groups) between sessions. The rats' behavior in the arena was monitored by an overhead video camera and activity was monitored utilizing Ethovision software. Two sessions, sample and test, were conducted each day. During the sample session, two identical objects were presented. During the test session, one object was replaced with an identical triplicate object while the other was replaced with an entirely novel object. Different objects were utilized for the no-delay and one-hour delay sessions. Exploration of an object is defined as directing the nose less than 2 cm to the object and actively exploring it. A discrimination index was calculated using the time spent exploring each object for each test session as ([novel object time–familiar object time]/ [novel object time + familiar object time]) to

control for differences in exploration duration.

Metabolic biomarker analysis

Glucose and insulin tolerance tests

Prior to both insulin and glucose tolerance tests (ITT/GTT), rats were fasted overnight, and there was a 48-hour washout period between ITT and GTT. Prior to injection, a small incision towards the end of the tail was made with a sterile surgical scalpel, and baseline (time 0) blood glucose levels were measured using an accu-check (Care Touch Blood Glucose Monitoring System). Rats were then immediately injected intraperitoneally with insulin (0.75 U/kg) or glucose (2 g/kg) and additional blood glucose values were obtained 15, 30, 60, and 90 min from the injection time.

Body composition analysis

Body composition was determined prior to behavioral analysis to avoid confounding effects of modest food restriction on fat mass. To determine body composition, time-domain nuclear magnetic resonance (TD-NMR) in restrained but awake and alert rats (TD-NMR Minispec, Bruker Optics) was used. Rats were placed into a sample holder which was then fit to their body size, secured with Velcro, and placed into the machine. Each scan lasted approximately 90 s and was run twice per animal. The average grams of lean body mass and fat mass from both runs was determined and compared against the body weight of the animal to determine lean and fat percent, respectively.

LC-MS analysis of fecal short chain fatty acids

Fecal samples (0.1 g) were lyophilized and 10 mg weighed portions were mixed with ice-cold methanol (2 mL) containing the internal standard $^{13}C_4$-butyric acid (0.05 ug/ml) to precipitate proteins [33]. The samples were centrifuged for 10 min at 14,000 × g and supernatants were collected. Each supernatant (80 µl) was added to 1-Ethyl-3-(3-dimethylaminopropyl) carbodiimide (10 µl, 0.25 M) and 10 µl of 0.1 M O-benzylhydroxylamine (o-BHA, 10 µl, 0.1 M) to chemically modify SCFAs with o-BHA. The resulting mixture was derivatized for 1 h at room temperature. Samples were diluted 20-fold in 50 % methanol. The diluted samples (200 µl) were subject to liquid–liquid extraction with dichloromethane (DCM, 600 µl). Samples were vortexed for 1 min and phases were allowed to separate. A portion of the DCM phase (40 µl) was transferred to a glass tube and dried under N_2 gas [34]. Samples were reconstituted in 30 % methanol (200 µl) and then transferred to loading vials. SCFA standards (MilliporSigma, CRM46957, Burlington, MA) were processed in the same manner as samples. Concentrations from 0.1–5,000 µM were used to create standard curves for each SCFA. Samples were analyzed by tandem HPLC-MS utilizing a 20A HPLC (Shimadzu, Kyoto, Japan) and an API 4000 triple quadrupole mass spectrophotometer (SCIEX, Framingham, MD). Instrument control and data acquisition utilized Analyst 1.6.2 (SCIEX). Authentic standards and samples were analyzed as previously described [53] with slight alterations. A Kinetex C_{18} reverse-phase column (2.6 µM 100 × 3.0 mm ID, Phenomenex, Torrance, CA) was employed for gradient separation. Mobile phase B was altered to 20 % isopropanol/80 methanol/0.1 % formic acid. MultiQuant 1.3.2 (SCIEX) was used for post-acquisition data analysis; peaks in all standards and plasma extracts were normalized to the $^{13}C_4$-butyric acid internal standard signal. Each standard curve was regressed linearly with $1/x^2$ weighting.

Alzheimer's disease-related pathology

Tissue collection

Rats were placed in a DecapiCone (DecapiCones®, Braintree Scientific Inc., Braintree, MA) and rapidly killed by decapitation. Brains were immediately extracted and hemisected. The left prefrontal cortex and hippocampus were isolated, and flash frozen in liquid nitrogen. Fecal samples were collected directly from the distal colon, placed in Para-Pak (Meridian Bioscience Inc., Cincinnati, OH, USA). A piece of each intestinal segment (duodenum, jejunum, ileum, and colon) was also isolated and stored in Para-Pak. All instruments and gloves were disinfected or changed between subjects and between tissue types within the same subject, though collections were under non-sterile conditions. All tissues were stored at −80 °C until use.

Protein quantification

Protein was quantified using an automated capillary electrophoresis based western blotting system (Jess, ProteinSimple, San Jose, CA, USA) in brain (hippocampus and prefrontal cortex) and intestinal (duodenum, jejunum, ileum and colon) samples. This system has been shown to be as (if not more) reliable than traditional western blotting [35]. Protein homogenate, extracted with Tissue Protein Extraction Reagent (T-PER; Thermo Scientific) and Halt Protease and Phosphatase Inhibitor Cocktail (Thermo Scientific), was mixed with the simple western sample buffer, denatured for 5 min at 95 °C and loaded onto the 12–230 kDa Jess Separation Module, 25 capillary cartridge (ProteinSimple, SM-W003) with the protein normalization module (ProteinSimple, DM-PN02). Target antibodies for β-Amyloid (β-Amyloid 1–16, clone 6E10, BioLegend Cat# 803002 and Aβ42, clone H31L21, ThermoFisher Cat# 700254) were diluted to 1:20. Phospho-Tau Thr231 (Invitrogen Cat# MN1020) was diluted1:10. The assay was completed per manufacturer's protocols, utilizing the Protein Normalization Module (cat# AM-PN01). Outputs were quantified via Compass, the accompanying software from ProteinSimple.

Statistical analysis

Behavioral analysis was conducted with an ANOVA by genotype or ANOVA-RM by genotype with the task type as a repeated factor. Biological variables, including weight, body fat, lean mass and fasted glucose were analyzed with an ANOVA by genotype. Metabolic tolerance tests were analyzed via ANOVA-RM across genotypes with timepoint as the repeated factor. Short chain fatty acid was analyzed as a 2-way ANOVA with genotype and SCFA as factors. Neuropathology was analyzed as 2-way ANOVAs with genotype and brain region as factors. Lifespan and WMBAT learning were assessed via Kaplan-Meier curve analysis. All analyses were performed with GraphPad Prism version 10.0.2 for Windows (GraphPad Software, San Diego, California USA, https://www.graphpad.com). Statistical significance was considered at p-values less than 0.05 unless otherwise stated. See below for details of microbiome analysis.

Microbiome analysis

Sample collection and microbiome analysis

At the conclusion of the behavioral test battery, animals were euthanized via rapid decapitation. A sample was collected from the duodenum, jejunum, ileum and colon and a fecal sample was removed directly from the distal colon. All samples were stored in commercially available preservative Para-Pak (Meridian Bioscience Inc., Cincinnati, OH), and immediately frozen and stored at −80 °C. Samples were processed for taxonomic analysis by the UAB Microbiome core as previously described [36,37]. Briefly, 16S-based polymerase chain reaction (PCR) procedures with unique bar-coded primers to amplify the V4 region of the 16S rRNA was utilized to create an amplicon library. Following electrophoresis, UV illumination as utilized to visualize the PCR product, which was excised and purified. Paired-end reads of approximately 250 bp from the V4 region of 16S rDNA were analyzed. Following quantitation with Pico Green, Fastq was utilized to convert raw data files after de-multiplexing. Sequences were grouped into amplicon sequence variants (ASV) and fecal microbiota composition and abundance were analyzed. ASVs were then filtered, clustered and summarized at different hierarchical levels (e.g., phylum, class, etc.). The taxonomic identification of the ASVs sequences was obtained using Mothur and compared with daSILVA 16S database. Data were analyzed utilizing R (version 4.3.0), primarily using the Phyloseq package in addition to *ape, genefilter, HTSSIP, and ggpicrust2* packages [38–43]. Alpha diversity was calculated utilizing the microbiome package in R [44], and beta diversity was calculated utilizing the Phyloseq package in R [38] via permutational multivariate analysis of variance (PERMANOVA). Analysis of Compositions of Microbiomes (ANCOM) with Bias Correction was used to test for differential abundance of microbial communities between groups using modified versions of previously published ANCOM scripts with a detection limit of 0.7 [45–47]. LEfSe method was utilized to explore differences between taxonomic groupings across genotypes [48]. Finally, PICRUSt2 was used to predict the abundance of functional pathways from 16S expression data, and to compare the abundance of these pathways between groups [49]. Briefly, PICRSt2 was executed in python using Mamba version 1.4.2, and PICRUSt2 version 2.3.0_b as downloaded from the bioconda repository, following instructions on the official PICRUSt2 github wiki. The full PICRUSt2 pipeline was then run using all defaults. Results of the PICRUSt2 analysis were analyzed for significantly differential expression of functional pathways using ALDEX2 and LinDA analyses as implemented in the R package *ggpicrust2*.

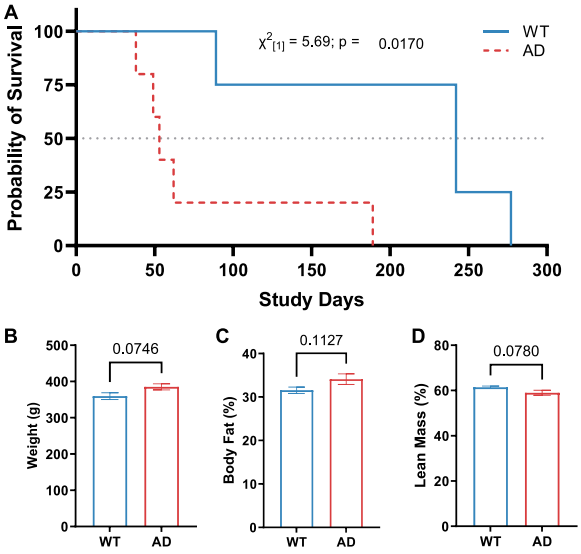

Fig. 2. TgF344-AD rats exhibited poorer health. (A) Lifespan was significantly shorter for TgF344-AD rats than their wildtype counterparts. There was also a trend for (B) higher body weight (p = 0.07), (B) higher body fat percentage (p = 0.11) and (C) lower lean mass percentage (p = 0.08), though none of these factors reached significance with the small sample size that survived until the end of the study. All data in B-D represent group means ± SEM.

CCA ordinations using vegan

Canonical correspondence analyses (CCA) of rarefied operational taxonomic unit (OTU) counts, PICRUSt2 predicted metabolic pathways, and behavioral, and biological predictors was carried out in R using version 2.5-7 of the *vegan* package [41]. This method allows for the exploration of correlations between OTU counts (or abundance of predicted metabolic pathways), and sample groups (here, samples were grouped by rat genotype), while also including outside explanatory variables as constraints on these correlations. Four CCAs were performed for this study. The first two included either behavioral scores (WMOD and WMBAT) and bodyweight as predictors, or amino acid concentration data as the predictors and OTUs as the outcomes. The second two included the same predictors, but used the PICRUSt2 predicted metabolic pathways as the outcomes. All CCAs allowed samples to be grouped by their genotype (Alzheimer's vs wild type). Correlations between OTUs/pathway abundances and samples were scaled with calculated eigenvalues (vegan::cca(scl = 3)). The significance of predictors in each CCA was tested using permutation tests (vegan::envfit(permutations = 999)).

Results

Lifespan and healthspan differ in TgF344-AD rats relative to wildtype

While only 5 wt and 5 TgAD rats survived through the end of the study and thus were included in all other data analysis, the study began with 9 wt and 10 TgAD rats. A survival analysis of all rats that did not reach the end of the study indicates the proportions significantly differed across genotype ($\chi^2_{[1]} = 5.69$; $p = 0.02$; Fig. 2A), such that WT rats survived significantly longer than TgAD rats.

Prior to food deprivation for behavioral analysis, there was a strong trend for TgAD rats to weigh more than their WT counterparts ($t_{[8]} = 2.05$; $p = 0.07$; Fig. 2B). Moreover, body composition analysis similarly indicated a trend towards TgAD rats having higher body fat percentage ($t_{[8]} = 1.78$; $p = 0.11$; Fig. 2C) and lower lean mass percentage ($t_{[8]} = 2.02$; $p = 0.08$; Fig. 2D) than their WT counterparts.

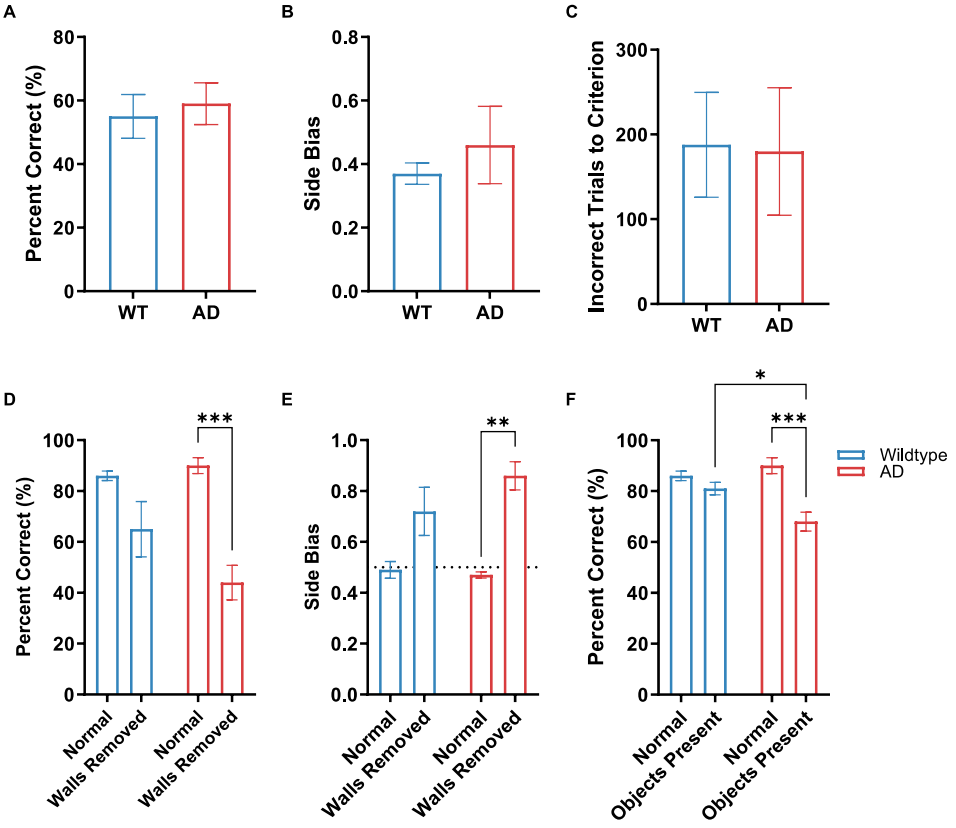

Fig. 3. Alternation ability in TgF344-AD rats is more affected by interfering stimuli than WT counterparts. There were no initial differences in interest or ability to alternate on the first day of exposure to the maze, as measured by both (A) percent correct turns and (B) side/turn bias. Moreover, (C) the number of incorrect trials performed until criterion alternation performance was reached did not differ. However, the removal of walls from one arm of the maze significantly impaired (D) percent correct turns and (E) side bias for TgF344-AD rats, but not WT rats, relative to their performance on the normal version of the task on the day prior. (F) Similarly, the first presentation of objects significantly impaired alternation ability in TgF344-AD rats, but not WT counterparts. All data represent group means ± SEM; * indicates $p \leq 0.05$, ** indicates $p \leq 0.01$, *** indicates $p \leq 0.001$.

TgF344-AD rats are cognitively impaired relative to wildtype

Ability to alternate is impaired in TgF344-AD rats with added interference, but not in wild type rats

On the first day of alternation training within the continuous alternation maze (CAM), there was no significant effect of genotype on the rats' innate ability to alternate between the two arms of the maze when comparing the percent of correct turns ($t_{[8]} = 0.42$; $p = 0.69$; Fig. 3A) nor the side bias ($t_{[8]} = 0.71$; $p = 0.50$; Fig. 3B). Moreover, the number of training trials rats underwent before learning to correctly alternate did not significantly differ across groups ($t_{[8]} = 0.08$; $p = 0.94$; Fig. 3C). These data suggest there are no differences in motivation to explore and alternate throughout the CAM without the interference of additional task measures.

To assess the influence of anxiety on the ability to correctly alternate throughout the CAM, the walls of one arm were removed and the rats were retested on alternation ability. Rats in both groups were performing equally well on alternations on the day prior to wall removal ($t_{[8]} = 1.09$; $p = 0.31$; Fig. 3D). However, when the walls were removed, the TgF344-AD rats performed significantly worse than the day prior ($t_{[16]} = 4.89$; $p = 0.001$), whereas the wildtype rats did not experience the same decline in performance ($t_{[16]} = 2.32$; $p = 0.22$). Prior to removing the walls, rats were not biased towards the arm in which walls would be removed ($p > 0.07$ for both groups; Fig. 3E). However, there was a significant effect of removing the walls on side bias ($F_{[1,16]} = 29.01$; $p < 0.001$). Post hoc analyses revealed that while TgF344-AD rats were significantly more biased towards the closed arm ($t_{[16]} = 4.79$; $p = 0.001$), wildtype rats were not significantly more biased towards the closed arm than they were when the walls were still present, though data trended towards significance ($t_{[16]} = 2.8$; $p = 0.07$).

In addition to assessing the effect of wall removal on alternation ability, the effect of introducing an object discrimination task on alternation performance was evaluated. Relative to the percent correct alternations on the day prior to the first object task (WM/OD), TgF344-AD rats alternated significantly worse ($t_{[16]} = 5.375$; $p < 0.001$), but WT rats did not ($t_{[16]} = 1.22$; $p = 0.81$; Fig. 3F). Moreover, TgF344-AD rats alternated significantly worse than their WT counterparts when objects were introduced ($t_{[16]} = 0.98$; $p = 0.92$), despite similar performance on the day prior ($t_{[16]} = 3.18$; $p = 0.03$). These data indicate that the cognitive performance of TgF344-AD rats was significantly more impaired by the removal of the walls than their wildtype counterparts.

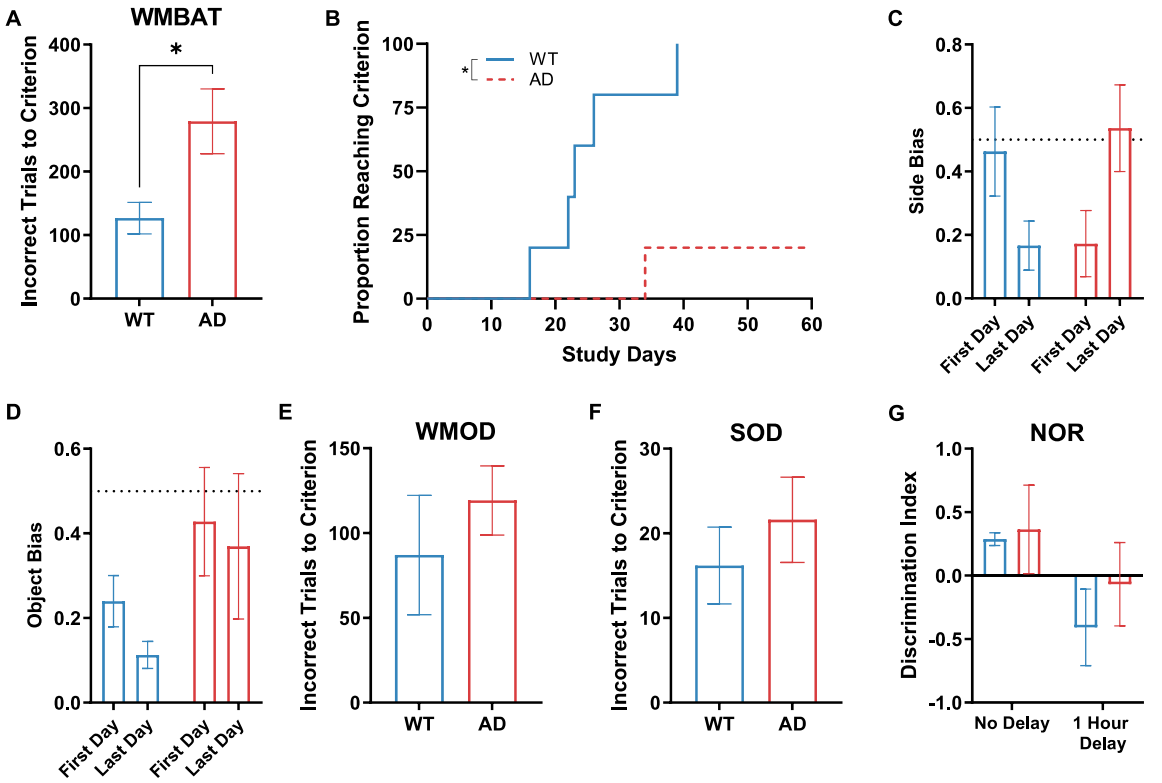

Fig. 4. TgF344-AD rats are impaired at associative learning, but not object recognition. (A) TgF344-AD rats required significantly more incorrect trials before reaching criterion performance on the working memory biconditional association (WMBAT) task. (B) In fact, most TgF344-AD rats did not reach criterion performance within the 60 training days allotted. (C) TgF344-AD rats adopt a more side-based bias during training, whereas (D) WT rats adopt an object-centric bias. (E) All rats, regardless of genotype, were able to complete an easier working memory object discrimination (WMOD) task, demonstrating that they were not only able to handle the walking load of the task, but the walking and alternating did not interfere with their ability to perform object discriminations in general. Similarly, (F) a simple object discrimination (SOD) task and a novel object discrimination (NOR) task did not indicate group differences, demonstrating a lack of physical inability to discriminate objects. All data represent group means ± SEM; * indicates $p \leq 0.05$.

TgF344-AD rats are impaired at complex associative tasks, but not object recognition and discrimination

To assess cognitive differences across genotypes, the working memory biconditional association task (WMBAT) was used. TgF344-AD rats required a significantly greater number of incorrect trials to reach a criterion performance than their wildtype counterparts ($t_{[8]} = 2.69$; $p = 0.03$; Fig. 4A). Moreover, only 1 out of 5 TgF344-AD rats was actually able to achieve criterion performance (≥80 % object choices correct on 2 consecutive days) within 60 days of training, whereas all wildtype rats achieved criterion within 40 days. Therefore, in addition to the aforementioned analysis that has been traditionally used to analyze learning on this specific task, a Kaplan-Meier curve was used to analyze behavioral performance, which also demonstrated significantly impaired performance in TgF344-AD rats relative to WT counterparts ($\chi^2 = 7.43$; $p = 0.006$; Fig. 4B).

While the wildtype rats demonstrated a bias towards a particular side on the first day of WMBAT training ($t_{[4]} = 3.295$, $p = 0.03$), this bias was insignificant on their final testing day ($t_{[4]} = 2.15$, $p = 0.10$), demonstrating their ability to overcome this biased strategy. Interestingly, TgF344-AD rats did not demonstrate a significant side bias on the first day ($t_{[4]} = 1.65$, $p = 0.17$), but became more biased throughout training such that on their final day of testing they were significantly biased towards one side ($t_{[4]} = 3.93$, $p = 0.02$; Fig. 4C). While both wildtype ($t_{[4]} = 3.96$; $p = 0.02$) and TgF344-AD rats ($t_{[4]} = 3.35$; $p = 0.03$) demonstrated a bias towards one particular object on day 1, this object-bias persisted on the final day of testing for the WT rats only ($t_{[4]} = 3.53$; $p = 0.02$) and not the TgF344-AD rats ($t_{[4]} = 2.15$; $p = 0.10$; Fig. 4D). Together, these data demonstrate that WT and TgF344-AD rats utilize different strategies for completing an associative object task.

To assess whether the alternation task increased the cognitive load so much so that rats are not able to do an easy object discrimination task, a working memory object discrimination (WMOD) task was administered. There was no significant effect of genotype on the number of incorrect trials required to reach criterion performance on this task ($t_{[8]} = 0.79$; $p = 0.45$; Fig. 4E), indicating that any differences observed in the more challenging WMBAT task were due to the cognitive load of the biconditional task and not from an inability to perform due to the interfering alternation task. The lack of difference in the average time to complete this task across groups ($t_{[4]} = 10.64$; $p = 0.29$; data not shown) also demonstrates no physical inability to perform a task requiring this amount of walking.

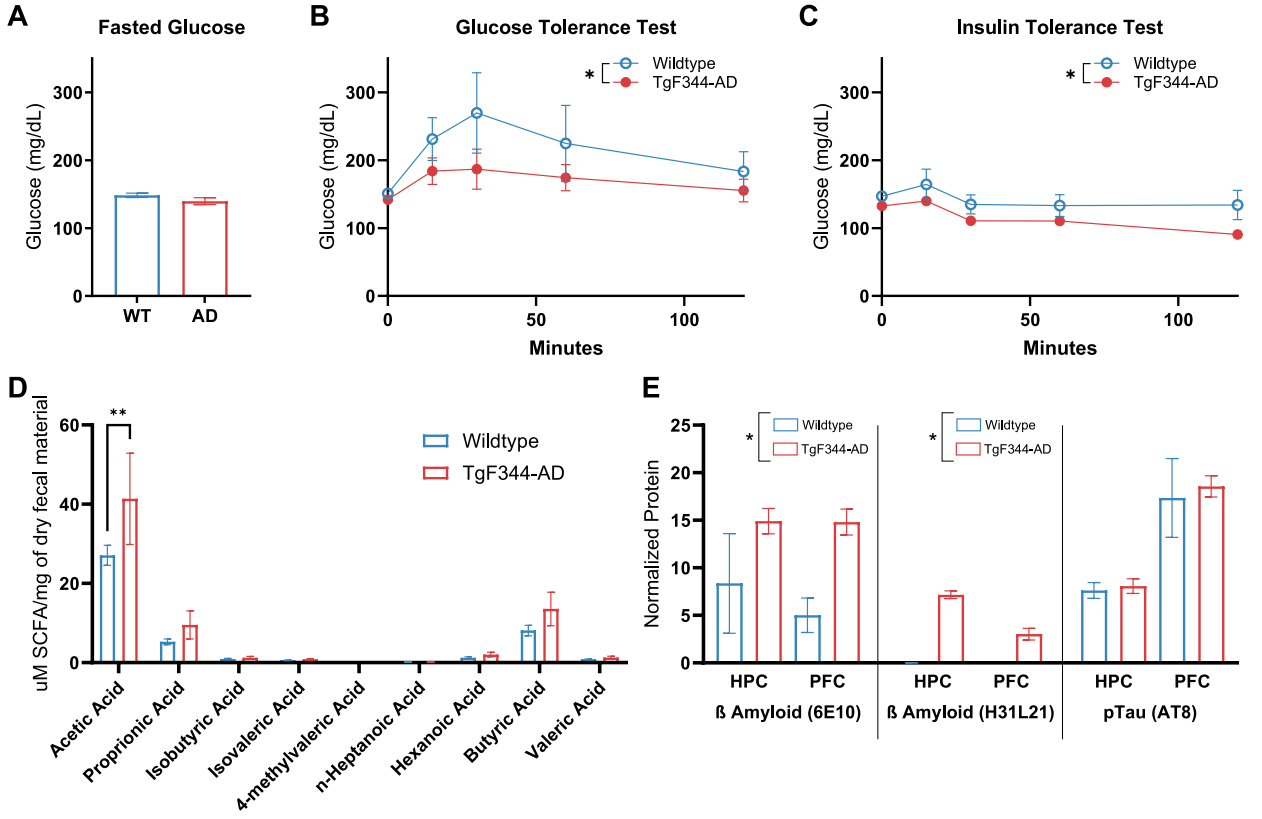

Fig. 5. TgF344-AD rats and WT counterparts exhibit altered metabolic processes. (A) While there was no difference in fasted glucose levels, both (B) glucose tolerance testing (GTT) and (C) Insulin Tolerance Testing (ITT) indicate altered glucose clearance in response to metabolic stimuli. (D) TgF344-AD rats had significantly higher levels of short chain fatty acids (SCFAs) in their feces than their WT counterparts. (E) Amyloid, but not pTau pathology, is significantly greater in TgF344-AD hippocampal (HPC) and prefrontal cortical (PFC) tissue than WT littermates. Amyloid deposition was significantly higher in TgF344-AD rats when quantified using both the 6E10 and H31L21 clones. Total Phosphorylated Tau (AT8 clone) did not differ in either brain region between TgF344-AD rats and WT littermates. All data represent group means ± SEM; * indicates $p \leq 0.05$, ** indicates $p \leq 0.01$.

To rule out the possibility that impairments in cognitive performance are due to an inability to see or discriminate between objects, several control tasks were conducted. A simple object discrimination (SOD) task in which rats are not required to perform the additional working memory task, and without a spatial component, was utilized. There were no significant effects across genotype on the

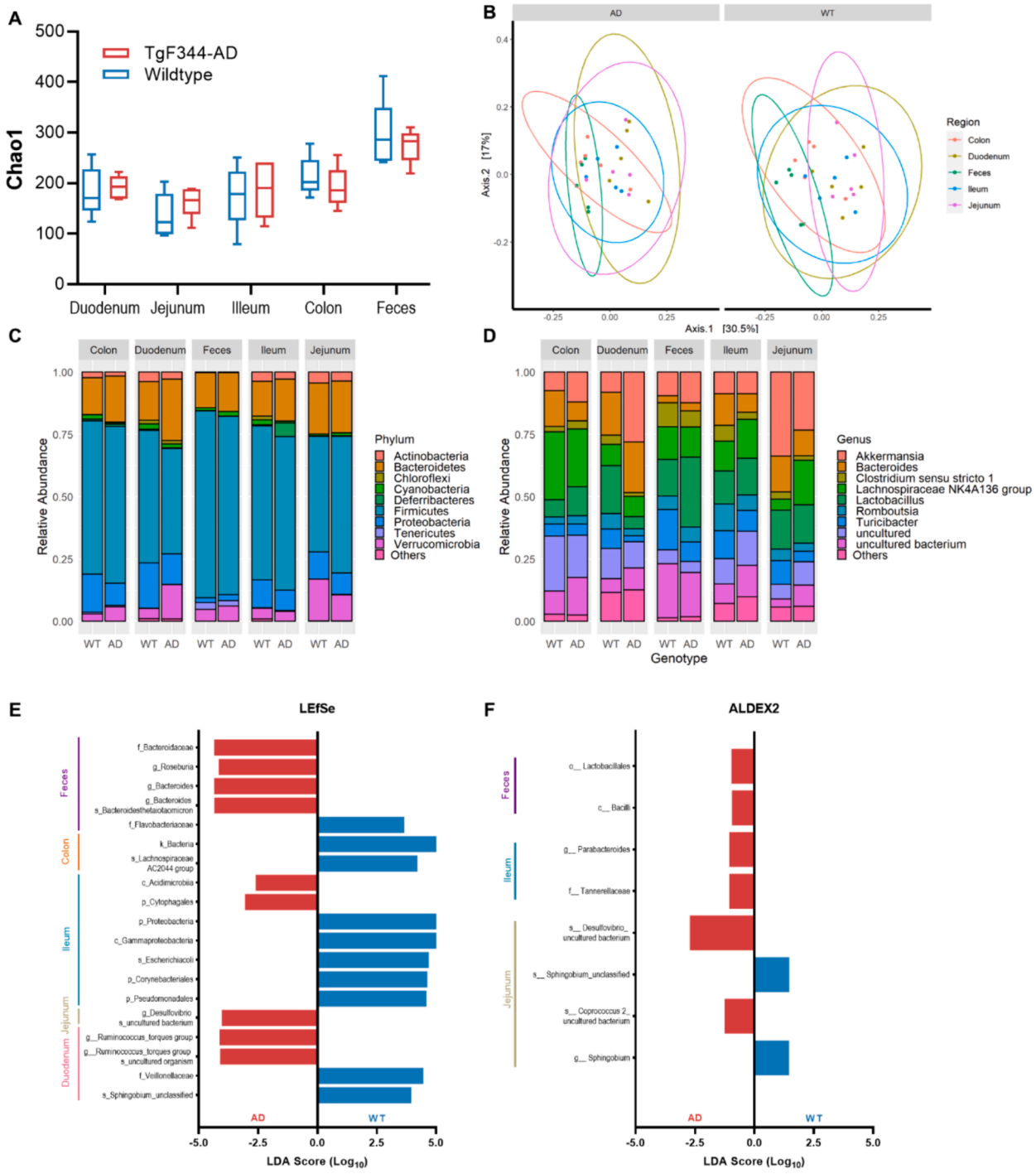

Fig. 6. Microbiome composition differs across intestinal region and genotype at 25 + months of age. (A) Chao1 index of alpha diversity significantly differed across intestinal region ($p < 0.001$), but not genotype ($p = 0.93$). (B) Similarly, beta diversity significantly differed by region ($p = 0.001$) but not genotype ($p = 0.21$). Several taxonomies significantly differed across genotype for specific regions at both the (C) phyla and (D) genera levels of taxonomic classification. (E) Linear Discriminant Analysis Effect Size (LEfSe) and ANOVA-like Differential Expression (ALDEX2) of the LDA scores computed for features differentially abundant between wildtype and TgF344-AD rats indicate regional specificity to differences observed.

SOD task ($t_{[8]} = 0.80$; $p = 0.45$; Fig. 4F), indicating no motor or physical impairments prevented rats of either genotype from successfully completing any of the object discrimination tasks. Finally, there were no differences in ability to recognize novel stimuli as determined by novel object recognition (NOR). When no delay was imposed, both WT and AD rats were able to recognize a novel object and there was no difference in performance across genotype ($t_{[11]} = 0.20$; $p > 0.99$; Fig. 4G). When a 1-hour delay was imposed, neither genotype was able to differentiate between the novel and familiar objects, again there was no difference in performance across genotypes ($t_{[11]} = 0.81$; $p = 0.97$).

TgF344-AD rats demonstrate a different metabolic phenotype than their wildtype counterparts

Glucose and insulin tolerance tests were conducted to assess peripheral metabolic health. The average fasted glucose level at time 0 was averaged across each test day for all rats, and there was no significant influence of genotype on baseline glucose ($t_{[8]} = 1.43$; $p = 0.19$; Fig. 5A). However, following an intraperitoneal injection of glucose, there was a significant effect of genotype on circulating glucose levels ($F_{[1,40]} = 4.54$, $p = 0.04$; Fig. 5B), though genotype did not significantly interact with timepoint ($F_{[4,40]} = 0.36$, $p = 0.83$), suggesting they did receive and respond to the glucose bolus. Similarly, the insulin injection resulted in significantly different responses across genotype ($F_{[1,30]} = 8.87$, $p < 0.01$; Fig. 5C) but genotype did not significantly interact with timepoint ($F_{[4,30]} = 0.31$, $p = 0.87$). While there was a significant effect of timepoint ($F_{[4,30]} = 2.70$, $p = 0.049$), the values obtained are lower than traditionally observed following ITT, indicating that the concentration utilized herein may have been insufficient to substantially drive glucose clearance.

As an additional measure of metabolic differences across genotypes, several short chain fatty acids were quantified from fecal waste. Not only were there significant differences in the quantity of each of the SCFAs analyzed ($F_{[8,63]} = 32.35$; $p < 0.01$), there was also a significant effect of genotype ($F_{[1,6]} = 4.88$; $p = 0.03$) such that TgF344-AD rats had significantly greater abundance than wildtype rats (Fig. 5A). However, this only reached significance in post hoc pairwise analyses for acetic acid ($t_{[63]} = 3.65$; $p < 0.01$) and no other SCFAs ($p > 0.81$ for all other comparisons).

TgF344-AD rats have increased amyloid, but not tau

Amyloid and Tau burden were assessed within the prefrontal cortex and hippocampus via protein quantification. For both amyloid antibodies utilized (Fig. 5E), TgF344-AD rats had significantly higher amyloid across both brain regions (6E10: $F_{[1,12]} = 7.77$; $p = 0.02$; H31L21: $F_{[1,12]} = 186.4$; $p < 0.001$). While there was no difference across PFC and HPC for the 6E10 clone ($F_{[1,12]} = 0.34$; $p = 0.57$), there was significantly higher amyloid deposition within the HPC for the H31L21 clone ($F_{[1,12]} = 31.09$; $p < 0.001$) than the PFC. pTau was not significantly different across genotypes in either region ($F_{[1,12]} = 0.14$; $p = 0.71$), though there was significantly higher levels of pTau within the PFC than the HPC ($F_{[1,12]} = 20.71$; $p < 0.001$; Fig. 5E). Our observation of relatively high AT8 in WT rats matches previous reports of age-related increases in phospho-tau [50].

TgF344-AD rats have region-specific gut dysbiosis

Gut microbiome diversity did not differ by genotype

Several measures of alpha diversity, or diversity across samples, were utilized to investigate regional and genotypic differences in microbiome composition. While Chao1, an estimate of total richness based on abundance, significantly differed across regions ($F_{[4,40]} = 11.48$; $p < 0.0001$), there was no significant main effect of genotype ($F_{[1,40]} = 0.01$; $p = 0.93$) and region did not significantly interact with genotype ($F_{[4,40]} = 0.52$; $p = 0.72$; Fig. 6A). Moreover, there were no significant effects of neither region nor genotype on Shannon or Simpson indices ($p > 0.38$ for all comparisons; data not shown).

Beta diversity, a measure of diversity within samples, was conducted using Unweighted UniFrac Analysis. PERMANOVA analysis revealed beta diversity significantly differed across intestinal region ($F_{[4,40]} = 5.27$; $p = 0.001$), but not genotype $F_{[1,40]} = 1.23$; $p = 0.21$) and there was no significant interaction between the two ($F_{[4,40]} = 0.66$; $p = 0.95$; Fig. 6B). Bray Curtis dissimilarity and Weighted UniFrac analyses revealed the same conclusions (data not shown).

Relative abundance significantly differs across genotype

Differences in taxonomic abundance across genotypes were investigated at the phylum (Fig. 6C) and genus (Fig. 6D) levels utilizing three different analyses, as differences in differential abundance methods vary within the same population [51]. Each region was examined independently, as diversity between regions significantly differed (see above). Firstly, differences in taxa across the two genotype groups were analyzed via Linear Discriminant Analysis Effect Size (LEfSe) [52] for each anatomical region. Significantly enriched taxa are described in Supplementary Table 1 and depicted in Fig. 6D.

Secondly, ANOVA-Like Differential Expression (ALDEX2) was utilized [53]. Significantly enriched taxa are described in Supplementary Table 1 and depicted in Fig. 6E. Importantly, for both methods, each intestinal region demonstrated unique changes in taxa, indicating that genotype-dependent changes in microbiome populations are specific to individual microbiome niches.

Lastly, Analysis of Compositions of Microbiomes (ANCOM) with Bias Correction was used to test for differentially expressed taxa across genotypes using modified versions of previously published ANCOM scripts with a detection limit of 0.7 [45–47,54]. However, regional analysis revealed no significant differences across genotypes for any taxa. Though a complete lack of effect was surprising, ANCOM is the most stringent of the three methodologies utilized [51]and thus it is logical it would yield the fewest differences among taxa. When ANCOM was run on all samples regardless of region, however, 11 phyla and 111 genera significantly differed across groups

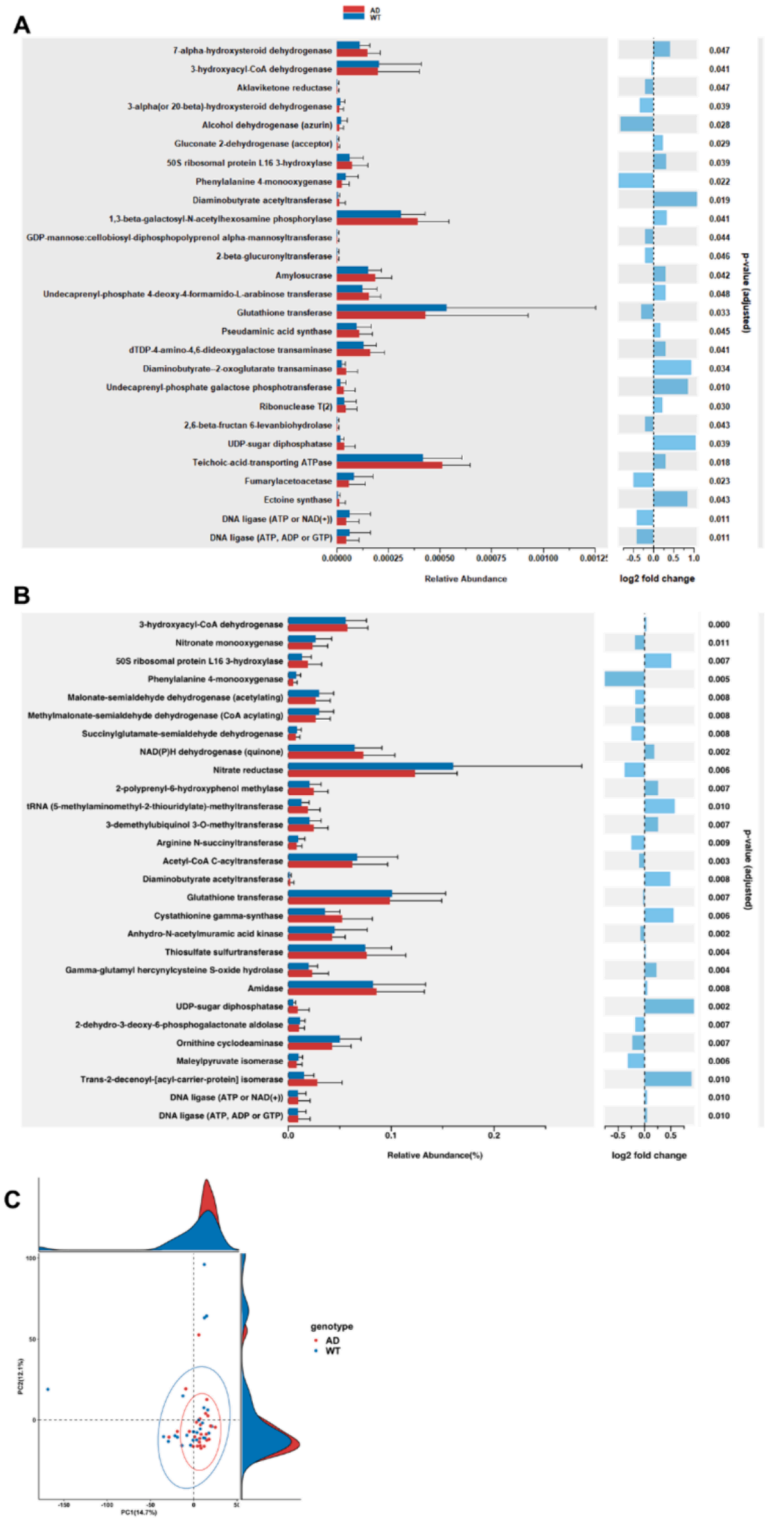

Fig. 7. Several functionally relevant enzyme classifications, found using MetaCyc database, were significantly altered by genotype as identified by (A) ALDEX2 and (B) LinDA. (C) PCA of enzyme pathway abundance by genotype.

(Supplementary Table 2).

Functional effects of gut microbiome alterations differed across genotype

While taxonomic differences are an important step in understanding genotype-specific shifts in gut microbe populations, the influence of these changes in functional outcomes is imperative to understanding the importance of these alterations. Therefore, marker gene sequences were utilized to predict functional abundances using Phylogenetic Investigation of Communities by Reconstruction of Unobserved States (PICRUSt2) [49] with the MetaCyc database [55]. As shown in Fig. 7, ALDEX2 (Fig. 7A) and LinDA (Fig. 7B) analyses revealed dozens of significantly altered enzyme pathways across genotype (only significantly altered pathways are shown), as well as significantly different pathway PCAs (Fig. 7C).

Several enzyme pathways of note were significantly altered across genotypes. Firstly, gut microbiome populations associated with the glutathione transferase enzyme pathway were significantly reduced in TgF344-AD rats relative to WT rats. This finding aligns with parallel findings in human AD patients, who display decreased glutathione transferase activity, as well as depleted levels of glutathione s-transferase protein, within the brain relative to age-matched control subjects [56]. Secondly, gut microbiome populations associated with the fumarylacetoacetase enzyme pathway are significantly decreased in TgF344-AD rats relative to their WT counterparts. These

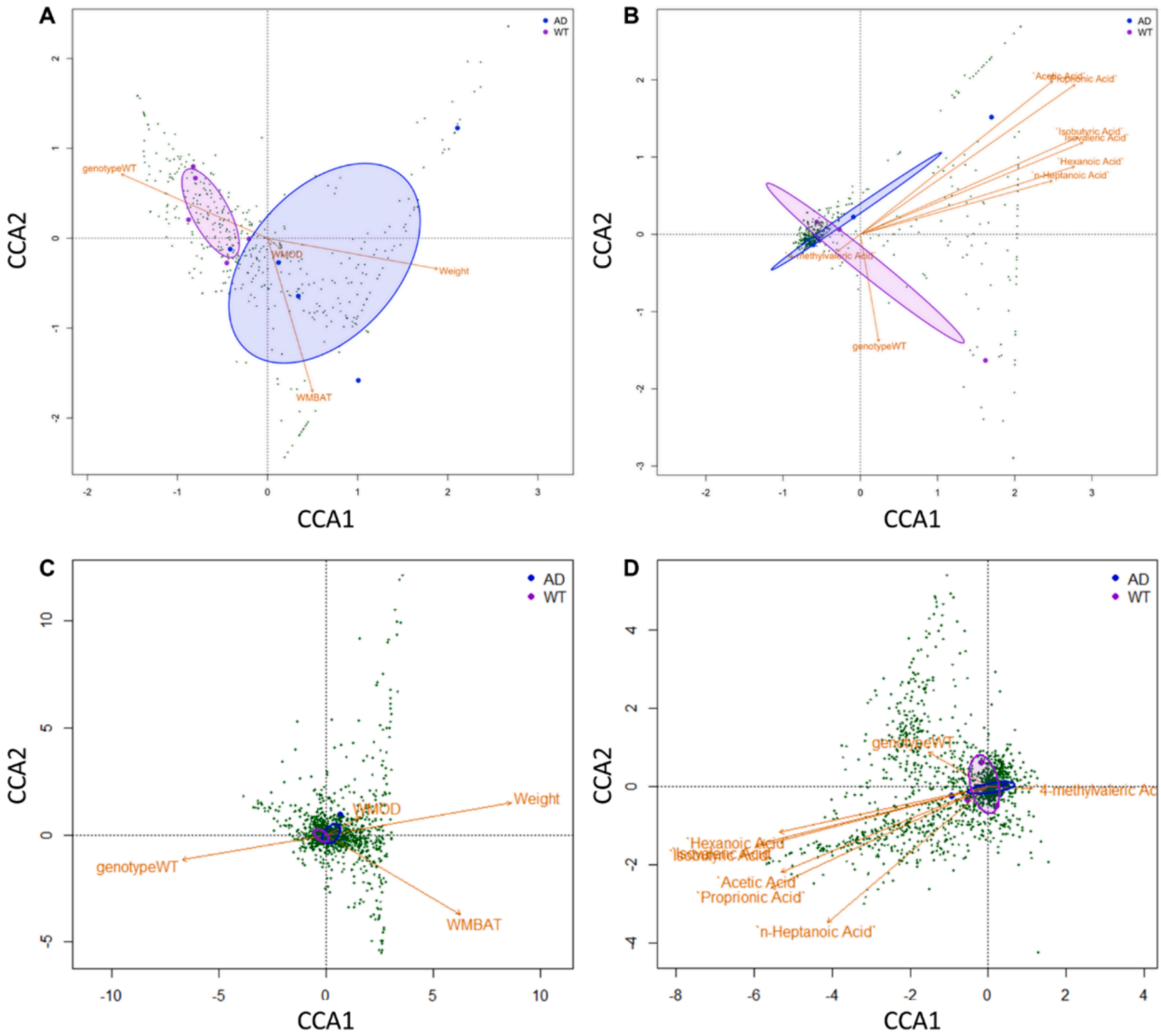

Fig. 8. A) CCA of genotype, bodyweight, WMOD, and WMBAT scores against OTU counts. B) CCA of genotype, and amino acid concentrations against OTU counts. C) CCA of genotype, bodyweight, WMOD, and WMBAT scores against metabolic pathways. D) CCA of genotype, and amino acid concentrations against metabolic pathways. Green points represent OTUs or metabolic pathways, blue and purple points and ellipses represent AD and WT samples and 95% confidence intervals respectively. (For interpretation of the references to colour in this figure legend, the reader is referred to the web version of this article.)

results again parallel humans with AD, as patients with late-onset Alzheimer's had a significant downregulation of the fumarylacetoacetate hydrolase domain containing 2A (FAHD2A) gene [57]. The FAHD2A gene is part of the larger FAH superfamily that plays a role in the degradation of tyrosine and phenylalanine, though the specific function of FAHD2A is not well-understood [58]. Thirdly, gut microbiome populations associated with the NAD(P)H dehydrogenase (quinone) pathway were significantly increased in TgF344-AD rats relative to WT rats. AD patients have a significantly increased ratio of frontal to cerebellar NAD(P)H Quinone Dehydrogenase 1 (NQO1) enzymatic activity compared to controls [59]. These findings indicate that the TgF344-AD rat model of AD is not only able to recapitulate cognitive and neuropathological effects of AD, but also alterations in metabolic function. Moreover, these alterations of previously unknown origins may be a direct result of altered gut microbiome composition.

CCA ordinations using vegan demonstrate relationships between operational taxonomic units/metabolic pathways and several key biological variables

Our ordinations showed significant relationships between both behavioral (Fig. 8A&C) and biological (Fig. 8B&D) variables and bacterial community structure. The first CCA (Fig. 8A) using behavioral variables on operational taxonomic unit (OTU) counts found that the first two canonical axes accounted for roughly 67 % of the variation observed in bacterial community structure, and this structure was found to be significantly related to both WMBAT scores ($p < 0.001$) and weight ($p < 0.001$), but not WMOD scores ($p = 0.969$). Rat genotype was also seen to significantly improve the fit of the model ($r^2 = 0.38$, $p = 0.007$). When the outcome was metabolic pathway (Fig. 8C), we saw similar results with the first two axes accounting for roughly 76 % of the variation, and both WMBAT ($p = 0.01$) and weight ($p < 0.001$) but not WMOD scores ($p = 0.868$) significantly explaining community structure, though rat genotype did not significantly improve model fit at the 0.05 α level ($r^2 = 0.27$, $p = 0.06$).

In our second CCA (Fig. 8B), using amino acid concentrations, the first two canonical axes accounted for roughly 45 % of the bacterial community variation, and we saw significant relationships between community structure and concentrations of Acetic ($p = 0.005$), Propionic ($p = 0.020$), Isobutyric ($p = 0.026$), Isovaleric ($p = 0.033$), Butyric ($p = 0.039$) and Valeric ($p = 0.015$) acids. However, we saw no significant effect of 4-methylvaleric ($p = 0.664$), n-Heptanoic ($p = 0.125$), or Hexanoic ($p = 0.063$) acids. Unlike the first model, we saw here that the inclusion of rat genotype did not significantly improve the fit of this model ($r^2 = 0.06$, $p = 0.688$). When the outcome was changed to metabolic pathway, we saw quite different results (Fig. 8D). The first two canonical axes represented roughly 75 % of metabolic pathway variation, and there was a significant relationship between metabolic pathway abundance and Proprionic acid ($p = 0.049$), but not Acetic ($p = 0.075$), Isobutyric ($p = 0.100$), Isovaleric ($p = 0.083$), Butyric ($p = 0.148$), Valeric ($p = 0.095$), 4-methylvaleric ($p = 0.609$), n-Heptanoic ($p = 0.141$), or Hexanoic ($p = 0.162$) acids. We also saw that rat genotype did not significantly improve model fit ($r^2 = < 0.01$, $p = 0.991$).

Discussion

Alzheimer's disease (AD) impacts neuropathology and cognitive function, as well as several periphral correlates, including metabolic impairment [2] and gut dysbiosis [3]. Gut health and microbiome composition play a large role in energy homeostasis, which in turn greatly influences cognition [5–7]. Thus, one potential avenue through which the gut may exert control over neurobiological health along the gut-brain-axis [8,9] is through regulation of metabolism, which strongly influences both of these organ systems [10,11]. Consequently, gut-derived impairments in peripheral and brain metabolism may underlie cognitive impairments associated with AD. Therefore, the current study examined associative memory, metabolic impairments and gut microbiome alterations in a rat model of AD bearing mutant human APP and PS1 (line TgF344-AD) [12].

Subjects utilized herein were all aged female rats, as aged females are the population are the most likely to suffer from AD and metabolic phenotypes in this rat model are sexually dimorphic [16]. While AD has long been associated with impaired metabolic processes, few rodent models have been shown to mimic neuropathological and cognitive impairments with metabolic perturbations. Moreover, it is currently underexplored whether the gut microbiome (GMB) influences the relationship between metabolic and neurobiological health.

Our data indicate that aged female TgF344-AD rats are impaired at the working memory biconditional association task (WMBAT). While their wildtype (WT) littermates were able to obtain the object-place association rule required for task completion, which is consistent with similarly aged rats from previously published work [20–22], the TgF344-AD rats were unable to do so. Cognitive differences were evident despite the challenges posed by the low survival rate known to occur in this model [60]. These data also demonstrate that while the WT rats progressively adopt a rule-based approach, the TgF344-AD rats demonstrate a location-based approach throughout training. This indicates TgF344-AD rats may not be able to adapt response strategies appropriately, such as utilizing an object-in-place rule, and perseverate on an unsuccessful strategy. While a strong side bias during early training is normal on this task [20], even aged subjects can typically overcome this bias to utilize an object-place association strategy to receive food reward [20,22], but not the TgF344-AD rats.

Moreover, TgF344-AD rats were significantly impacted by the addition of objects into the maze, as their previously acquired ability to correctly alternate was significantly impaired by the addition of these objects, which was not the case for WT rats. This impairment can be interpreted in several ways. Firstly, the increased cognitive load of a second task (alternation + object discrimination) could be too high a burden for the TgF344-AD rats to overcome. A second possibility is that while WT rats were still able to hold recent memories of location in mind, the investigation of objects caused too much interference in the TgF344-AD rats' working memory to maintain this information. While less cognitively challenging tasks, such as novel object recognition (NOR) are widely used in rodent studies, high variability across a low number of trials means the number of subjects required to detect differences in recognition memory is often insurmountably high [61]. While other aged rats can perform NOR with a one-hour delay, our WT rats were not able to

demonstrate recognition memory at this timepoint, though all rats were successful when no delay was imposed. These data demonstrate recognition memory on simple object discrimination tasks does not differ across groups. This reinforces the notion that more cognitively challenging tasks, such as WMBAT, are more appropriately attuned to detect cognitive differences in aging and age-related disease [20].

In addition to cognitive differences, in aged, female TgF344 rats, peripheral metabolism is impaired. While body weight and body fat percentage did not reach statistical significance across groups in this cohort, there were strong trends for TgF344-AD rats to be fatter than their WT counterparts. These data are in line with previous reports of excess weight and body fat in female TgF344-AD rats at younger ages, who also demonstrated impaired glucose clearance and reduced insulin sensitivity [15,16]. Intriguingly, despite poorer peripheral health overall, this specific cohort of rats did not demonstrate impaired glucose clearance. This is in contrast to other cohorts in our lab and published by others, as well as in contrast to data demonstrating hypometabolism utilizing FDG-PET [16,62]. This may indicate that cognitive and enzymatic impairments are present prior to overt peripheral metabolic impairment in these subjects. Conversely, this may indicate that these subjects exhibit an enhanced level of glucose clearance as a compensatory mechanism for declining peripheral and metabolic health, which is no longer feasible at later ages. Our data also demonstrate significantly higher amyloid within the hippocampus and prefrontal cortex of these subjects relative to WT controls as previously established [12]. However, no significant tau (AT8) burden was observed in our subjects as others have also previously reported [12,63].

In line with established alterations in GMB composition within human AD patients [64–66], we observed significant alterations in GMB composition within the TgF344-AD rats relative to their WT counterparts. Intriguingly, many of the microbes that are significantly reduced in the ileum of TgF344-AD rats are known to be pro-inflammatory, including Proteobacteria [67], Gammaproteobacteria [68], Escherichia coli [69], and Pseudomonas [70]. This may suggest that regionally specific microbial subpopulations in TgF344-AD rats reorganize in a compensatory fashion. It is possible that TgF344-AD rats have earlier impairments in microbial function that are overcompensated for in later adulthood, but the WT rats slowly experience altered dysbiosis with increasing age-related inflammation. Interestingly, the only other group to previously report of GMB alterations in this model reported an increase in the genus Lachnoclostridium, an anti-inflammatory microbe [71], in male TgF344-AD rats at 14 months of age [30]. Future longitudinal studies can further assess the time course of these regionally specific alterations in microbial populations as well as investigate the relationship between these microbes and degree of inflammation across tissue types and in the circulation. While alterations in diversity and specific taxa have been previously published in this transgenic model [30], we have expanded upon this data by including GMB populations from not only fecal samples, but also several intestinal segments (duodenum, jejunum ileum and colon). As predicted, the microbial populations within each intestinal segment significantly differed. Not only do fecal and intestinal metabolomes differ significantly in humans [72], but the functional relevance of alterations across different intestinal regions have implications for the altered metabolism observed in AD. Fecal microbiome populations are largely representative of colonic GMB composition and thus do not indicate whether alterations within other intestinal segments occur. This is particularly important in AD, as patients with dementia demonstrate an increased preference for a high carbohydrate diet [27,73] as well as an impaired ability to metabolize carbohydrates [74], which takes place in the small intestine [75]. Nutritional metabolism can regulate brain bioenergetics, influencing AD-risk [76]. Increased carbohydrate consumption is also associated with higher degrees of neuropathology [77] and poorer cognitive performance [78]. Moreover, the undigested fiber products that make it past the small intestine are converted to short chain fatty acids (SCFA) in the large intestine by a distinct set of gut microbes [79]. Alterations in the GMB populations specifically contributing to these functions would be missed with fecal sample analysis alone.

Our data also expands upon the previous work through the use of aged female subjects, which have not yet been explored in this manner. Sex is not only an important factor in AD, but changes in GMB populations are sex dependent, particularly when exploring the relationship between visceral fat and GMB [80]. Advanced age is also associated with shifts in GMB composition [81]. Additionally, our analysis not only includes descriptive taxonomic classification, but includes a prediction of functional alterations as a result of the altered GMB population, which has not been explored in this model for any age or sex. There is evidence of reduced glucose utilization in AD subjects within affected brain regions [82,83], often referred to as brain hypometabolism, which is thought to occur early in the disease process. This may impair the function of dehydrogenases involved in glucose metabolism, such as those in the glycolytic pathway and the pentose phosphate pathway. Therefore, we utilized PICRUSt2 to investigate changes in enzyme pathways via MetaCyc, which determined several significantly affected pathways, indicating metabolism may be an intermediary process between the gut and brain in neurodegeneration. This analysis demonstrates that the alterations in GMB observed in the TgF344-AD rats, relative to their WT counterparts, can directly influence metabolism. Several enzyme pathways that significantly affect metabolic function systemically were significantly different across groups (see Fig. 7).

Notably, several of these alterations may impact neurotransmitter levels, which can influence neuronal signaling and therefore neurobiological function. For example, the Phenylalanine 4-monooxygenase pathway was significantly downregulated in AD rats, which could indicate decreased levels of dopamine or other catecholamines, as this enzyme is critical for the conversion of phenylalanine to tyrosine. Additionally, alterations in nitrate reductase can influence nitric oxide levels, which also has implications for altered neurotransmission. Succinylglutamate-semialdehyde dehydrogenase (SGSD), which is involved in the catabolism of lysine, was also downregulated in AD rats. In addition to its influence on neurotransmitter levels, SGSD can influence glucose metabolism. In fact, several of these dysregulated pathways are critical for metabolism of energy sources required for neurons to fire, including gluconate 2-dehydrogenase, UDP-sugar diphosphatase, Malonate-semialdehyde dehydrogenase (acetylating) and NAD(P)H dehydrogenase (quinone). Lastly, DNA ligase (ATP or NAD(+)) pathway activity was significantly altered by genotype. While not directly involved in glucose metabolism, altered DNA repair processing may have implications for many avenues of cellular function, including metabolic processes.

Following the characterization of the gut microbiome composition, the relationship between observed changes in operational

taxonomic units (OTUs) with behavioral and biological variables were assessed via canonical correspondence analyses (CCA). These analyses demonstrate genotype, cognition, and body weight all significantly related to bacterial community structure. Moreover, bacterial community variation was also significantly related to concentrations of several short chain fatty acids in fecal samples. These data suggest that not only is there gut dysbiosis occurring in aged TgF334-AD rats, but that these alterations are in fact related to the behavioral and metabolic phenotypes observed.

This work was limited by several factors, including the fact that this animal model is a model of familial AD, whilst the vast majority of AD cases are sporadic. Alterations in the GMB of AD patients are independent of genotype [84], suggesting there is more to gut dysbiosis in AD than presented herein. Secondly, the decreased lifespan of these rats may inhibit the ability to assess the interaction of aging with the expression of AD-related genes. Cross breeding the TgF344-AD rats with Brown Norway rats may provide a heartier model of AD in a FBN-AD-F1 rat. While future work could benefit from increased subjects, particularly both males and females throughout the lifespan, the data described herein lay the groundwork for leveraging the GMB in AD-related treatments, as these types of interventions are more easily translatable to human populations than pharmacological interventions targeting brain function directly.

Funding sources

This research was funded by the National Institute on Aging of the National Institutes of Health Award # 1K99AG078402-01 (ARH) and # P30 AG050886 (ARH), partially supported by #5K02AG062498 (TWB), and was made possible by the UAB Center for Clinical and Translational Science Grant #UL1TR001417 from the National Center for Advancing Translational Sciences (NCATS) of the National Institutes of Health (NIH). The content is solely the responsibility of the authors and does not necessarily represent the official views of the National Institutes of Health.

CRediT authorship contribution statement

Abbi R. Hernandez: Writing – review & editing, Writing – original draft, Visualization, Resources, Project administration, Methodology, Investigation, Funding acquisition, Formal analysis, Data curation, Conceptualization. **Erik Parker:** Writing – review & editing, Visualization, Formal analysis. **Maham Babar:** Writing – review & editing, Investigation. **Anisha Banerjee:** Project administration, Investigation. **Sarah Ding:** Investigation. **Alexis Simley:** Investigation. **Thomas W. Buford:** Writing – review & editing, Supervision.

Declaration of competing interest

The authors declare that they have no known competing financial interests or personal relationships that could have appeared to influence the work reported in this paper.

Acknowledgements

Taylor Berryhill and the UAB Targeted Metabolomics and Proteomics Laboratory and its instruments (purchase of the SCIEX 4000 mass spectrometer in the Targeted Metabolomics and Proteomics Laboratory came from funds provided by the UAB Health Services Foundation General Endowment Fund) and the UAB Microbiome Resource.

Appendix A. Supplementary data

Supplementary data to this article can be found online at https://doi.org/10.1016/j.nbas.2024.100119.

References

[1] What is Alzheimer's Disease? | CDC 2021. https://www.cdc.gov/aging/aginginfo/alzheimers.htm (accessed July 9, 2021).
[2] Arvanitakis Z, Wilson RS, Bienias JL, Evans DA, Bennett DA. Diabetes mellitus and risk of alzheimer disease and decline in cognitive function. Arch Neurol 2004; 61:661. https://doi.org/10.1001/archneur.61.5.661.
[3] Hernandez AR, Banerjee A, Carter CS, Buford TW. Angiotensin (1–7) expressing probiotic as a potential treatment for dementia. Front Aging 2021;2. https://doi.org/10.3389/fragi.2021.629164.
[4] Chandra S, Sisodia SS, Vassar RJ. The gut microbiome in Alzheimer's disease: what we know and what remains to be explored. Mol Neurodegener 2023;18:9. https://doi.org/10.1186/s13024-023-00595-7.
[5] Hoyer S. Causes and consequences of disturbances of cerebral glucose metabolism in sporadic alzheimer disease: therapeutic implications. In: Vécsei L, editor. Frontiers in clinical neuroscience, Boston, MA: Springer US; 2004, p. 135–52. https://doi.org/10.1007/978-1-4419-8969-7_8.
[6] Ryan CM, Freed MI, Rood JA, Cobitz AR, Waterhouse BR, Strachan MWJ. Improving metabolic control leads to better working memory in adults with type 2 diabetes. Diabetes Care 2006;29:345–51. https://doi.org/10.2337/diacare.29.02.06.dc05-1626.
[7] Taylor VH, MacQueen GM. Cognitive dysfunction associated with metabolic syndrome. Obes Rev 2007;8:409–18. https://doi.org/10.1111/j.1467-789X.2007.00401.x.
[8] Proctor C, Thiennimitr P, Chattipakorn N, Chattipakorn SC. Diet, gut microbiota and cognition. Metab Brain Dis 2017;32:1–17. https://doi.org/10.1007/s11011-016-9917-8.

[9] Naveed M, Zhou Q-G, Xu C, Taleb A, Meng F, Ahmed B, et al. Gut-brain axis: A matter of concern in neuropsychiatric disorders…! Prog Neuropsychopharmacol Biol Psychiatry 2021;104:110051. https://doi.org/10.1016/j.pnpbp.2020.110051.
[10] Ott V, Benedict C, Schultes B, Born J, Hallschmid M. Intranasal administration of insulin to the brain impacts cognitive function and peripheral metabolism. Diabetes Obes Metab 2012;14:214–21. https://doi.org/10.1111/j.1463-1326.2011.01490.x.
[11] Utzschneider KM, Kratz M, Damman CJ, Hullarg M. Mechanisms linking the gut microbiome and glucose metabolism. J Clin Endocrinol Metab 2016;101: 1445–54. https://doi.org/10.1210/jc.2015-4251.
[12] Cohen RM, Rezai-Zadeh K, Weitz TM, Rentsendorj A, Gate D, Spivak I, et al. A transgenic Alzheimer rat with plaques, tau pathology, behavioral impairment, oligomeric aβ, and frank neuronal loss. J Neurosci 2013;33:6245–56. https://doi.org/10.1523/JNEUROSCI.3672-12.2013.
[13] Rorabaugh JM, Chalermpalanupap T, Botz-Zapp CA, Fu VM, Lembeck NA, Cohen RM, et al. Chemogenetic locus coeruleus activation restores reversal learning in a rat model of Alzheimer's disease. Brain 2017;140:3023–38. https://doi.org/10.1093/brain/awx232.
[14] Pentkowski NS, Berkowitz LE, Thompson SM, Drake EN, Olguin CR, Clark BJ. Anxiety-like behavior as an early endophenotype in the TgF344-AD rat model of Alzheimer's disease. Neurobiol Aging 2018;61:169–76. https://doi.org/10.1016/j.neurobiolaging.2017.09.024.
[15] Hernandez CM, Jackson NL, Hernandez AR, McMahon LL. Impairments in fear extinction memory and basolateral amygdala plasticity in the TgF344-AD rat model of Alzheimer's disease are distinct from non-pathological aging. Neuroscience 2022. https://doi.org/10.1101/2022.03.12.484093.
[16] Srivastava H, Lasher AT, Nagarajan A, Sun LY. Sexual dimorphism in the peripheral metabolic homeostasis and behavior in the TgF344-AD rat model of Alzheimer's disease. Aging Cell n.d.;n/a:e13854. https://doi.org/10.1111/acel.13854.
[17] Proskauer Pena SL, Mallouppas K, Oliveira AMG, Zitricky F, Nataraj A, Jezek K. Early spatial memory impairment in a double transgenic model of Alzheimer's disease TgF-344 AD. Brain Sci 2021;11:1300. https://doi.org/10.3390/brainsci11101300.
[18] Hernandez AR, Burke SN. Age-related changes in "hub" neurons. Aging 2018;10:2551–2. https://doi.org/10.18632/aging.101606.
[19] Sun Q, Zhang J, Li A, Yao M, Liu G, Chen S, et al. Acetylcholine deficiency disrupts extratelencephalic projection neurons in the prefrontal cortex in a mouse model of Alzheimer's disease. Nat Commun 2022;13:998. https://doi.org/10.1038/s41467-022-28493-4.
[20] Hernandez AR, Maurer AP, Reasor JE, Turner SM, Barthle SE, Johnson SA, et al. Age-related impairments in object-place associations are not due to hippocampal dysfunction. Behav Neurosci 2015;129:599–610. https://doi.org/10.1037/bne0000093.
[21] Hernandez AR, Hernandez CM, Campos K, Truckenbrod L, Federico Q, Moon B, et al. A ketogenic diet improves cognition and has biochemical effects in prefrontal cortex that are dissociable from hippocampus. Front Aging Neurosci 2018;10:391. https://doi.org/10.3389/fnagi.2018.00391.
[22] Hernandez AR, Truckenbrod LM, Campos KT, Williams SA, Burke SN. Sex differences in age-related impairments vary across cognitive and physical assessments in rats. Behav Neurosci 2020;134:69–81. https://doi.org/10.1037/bne0000352.
[23] Hernandez AR, Truckenbrod LM, Barrett ME, Lubke KN, Clark BJ, Burke SN. Age-related alterations in prelimbic cortical neuron arc expression vary by behavioral state and cortical layer. Front Aging Neurosci 2020;12. https://doi.org/10.3389/fnagi.2020.588297.
[24] Bachman DL, Wolf PA, Linn R, Knoefel JE, Cobb J, Belanger A, et al. Prevalence of dementia and probable senile dementia of the Alzheimer type in the Framingham Study. Neurology 1992;42:115–9. https://doi.org/10.1212/wnl.42.1.115.
[25] Fratiglioni L, Viitanen M, von Strauss E, Tontodonati V, Herlitz A, Winblad B. Very old women at highest risk of dementia and Alzheimer's disease: incidence data from the Kungsholmen Project, Stockholm. Neurology 1997;48:132–8. https://doi.org/10.1212/wnl.48.1.132.
[26] Gambassi G, Lapane KL, Landi F, Sgadari A, Mor V, Bernabie R. Gender differences in the relation between comorbidity and mortality of patients with Alzheimer's disease. Systematic Assessment of Geriatric drug use via Epidemiology (SAGE) Study Group. Neurology 1999;53:508–16. https://doi.org/10.1212/wnl.53.3.508.
[27] Mungas D, Cooper JK, Weiler PG, Gietzen D, Franzi C, Bernick C. Dietary preference for sweet foods in patients with dementia. J Am Geriatr Soc 1990;38: 999–1007. https://doi.org/10.1111/j.1532-5415.1990.tb04423.x.
[28] Davis CP. Normal flora. In: Baron S, editor. Medical microbiology. 4th ed. Galveston (TX): University of Texas Medical Branch at Galveston; 1996.
[29] Ahn J-S, Lkhagva E, Jung S, Kim H-J, Chung H-J, Hong S-T. Fecal microbiome does not represent whole gut microbiome. Cell Microbiol 2023;2023:e6868417. https://doi.org/10.1155/2023/6868417.
[30] Nagarajan A, Srivastava H, Reid R, Morrow CD, Sun L. Insights into the gut microbiota changes associated with Alzheimer's disease and aging in the Tgf344-AD rat model 2021.
[31] Cuervo-Zanatta D, Garcia-Mena J, Perez-Cruz C. Gut Microbiota alterations and cognitive impairment are sexually dissociated in a transgenic mice model of Alzheimer's disease. JAD 2021;82:S195–214. https://doi.org/10.3233/JAD-201367.
[32] Hernandez AR, Winesett SP, Federico QP, Williams SA, Burke SN, Clark DJ. A Cross-species model of dual-task walking in young and older humans and rats. Front Aging Neurosci 2020;12:276. https://doi.org/10.3389/fnagi.2020.00276.
[33] Hsu Y-L, Chen C-C, Lin Y-T, Wu W-K, Chang L-C, Lai C-H, et al. Evaluation and optimization of sample handling methods for quantification of short-chain fatty acids in human fecal samples by GC–MS. J Proteome Res 2019;18:1948–57. https://doi.org/10.1021/acs.jproteome.8b00536.
[34] Zeng M, Cao H. Fast quantification of short chain fatty acids and ketone bodies by liquid chromatography-tandem mass spectrometry after facile derivatization coupled with liquid-liquid extraction. J Chromatogr B 2018;1083:137–45. https://doi.org/10.1016/j.jchromb.2018.02.040.
[35] Sormunen A, Koivulehto E, Alitalo K, Saksela K, Laham-Karam N, Ylä-Herttuala S. Comparison of automated and traditional Western blotting methods. Methods Protoc 2023;6:43. https://doi.org/10.3390/mps6020043.
[36] Buford TW, Sun Y, Roberts LM, Banerjee A, Peramsetty S, Knighton A, et al. Angiotensin (1–7) delivered orally via probiotic, but not subcutaneously, benefits the gut-brain axis in older rats. GeroScience 2020. https://doi.org/10.1007/s11357-020-00196-y.
[37] Buford TW, Carter CS, VanDerPol WJ, Chen D, Lefkowitz EJ, Eipers P, et al. Composition and richness of the serum microbiome differ by age and link to systemic inflammation. GeroScience 2018;40:257–68. https://doi.org/10.1007/s11357-018-0026-y.
[38] McMurdie PJ, Holmes S. phyloseq: An R package for reproducible interactive analysis and graphics of microbiome census data. PLoS One 2013;8:e61217. https://doi.org/10.1371/journal.pone.0061217.
[39] Paradis E, Schliep K. ape 5.0: an environment for modern phylogenetics and evolutionary analyses in R. Bioinformatics 2019;35:526–8. https://doi.org/10.1093/bioinformatics/bty633.
[40] Youngblut ND, Barnett SE, Buckley DH. HTSSIP: An R package for analysis of high throughput sequencing data from nucleic acid stable isotope probing (SIP) experiments. PLoS One 2018;13:e0189616. https://doi.org/10.1371/journal.pone.0189616.
[41] Oksanen J, Blanchet F, Friendly M, Kindt R, Legendre P, McGlinn D, et al. Vegan: Commmunity Ecology Package. 2017.
[42] R. Gentleman VC. genefilter 2017. https://doi.org/10.18129/B9.BIOC.GENEFILTER.
[43] Yang C, Mai J, Cao X, Burberry A, Cominelli F, Zhang L. ggpicrust2: an R package for PICRUSt2 predicted functional profile analysis and visualization. Bioinformatics 2023;39:btad470. https://doi.org/10.1093/bioinformatics/btad470.
[44] Shetty SA, Lahti L. Microbiome data science. J Biosci 2019;44:115.
[45] Hernandez AR, Kemp KM, Burke SN, Buford TW, Carter CS. Influence of aging, macronutrient composition and time-restricted feeding on the Fischer344 x brown norway rat gut microbiota. Nutrients 2022;14:1758. https://doi.org/10.3390/nu14091758.
[46] Mandal S, Van Treuren W, White RA, Eggesbø M, Knight R, Peddada SD. Analysis of composition of microbiomes: a novel method for studying microbial composition. Microb Ecol Health Dis 2015:26. https://doi.org/10.3402/mehd.v26.27663.
[47] Kemp KM, Colson J, Lorenz RG, Maynard CL, Pollock JS. Early life stress in mice alters gut microbiota independent of maternal microbiota inheritance. Am J Physiol-Regul Integr Compar Physiol 2021;320:R663–74. https://doi.org/10.1152/ajpregu.00072.2020.
[48] Segata N, Waldron L, Ballarini A, Narasimhan V, Jousson O, Huttenhower C. Metagenomic microbial community profiling using unique clade-specific marker genes. Nat Methods 2012;9:811–4. https://doi.org/10.1038/nmeth.2066.
[49] Douglas GM, Maffei VJ, Zaneveld JR, Yurgel SN, Brown JR, Taylor CM, et al. PICRUSt2 for prediction of metagenome functions. Nat Biotechnol 2020;38:685–8. https://doi.org/10.1038/s41587-020-0548-6.

[50] Stranahan AM, Haberman RP, Gallagher M. Cognitive decline is associated with reduced reelin expression in the entorhinal cortex of aged rats. Cereb Cortex 2011;21:392–400. https://doi.org/10.1093/cercor/bhq106.

[51] Nearing JT, Douglas GM, Hayes MG, MacDonald J, Desai DK, Allward N, et al. Microbiome differential abundance methods produce different results across 38 datasets. Nat Commun 2022;13:342. https://doi.org/10.1038/s41467-022-28034-z.

[52] Segata N, Izard J, Waldron L, Gevers D, Miropolsky L, Garrett WS, et al. Metagenomic biomarker discovery and explanation. Genome Biol 2011;12:R60. https://doi.org/10.1186/gb-2011-12-6-r60.

[53] Fernandes AD, Reid JN, Macklaim JM, McMurrough TA, Edgell DR, Gloor GB. Unifying the analysis of high-throughput sequencing datasets: characterizing RNA-seq, 16S rRNA gene sequencing and selective growth experiments by compositional data analysis. Microbiome 2014;2:15. https://doi.org/10.1186/2049-2618-2-15.

[54] Hernandez AR, Watson C, Federico QP, Fletcher R, Brotgandel A, Buford TW, et al. Twelve months of time-restricted feeding improves cognition and alters microbiome composition independent of macronutrient composition. Nutrients 2022;14:3977. https://doi.org/10.3390/nu14193977.

[55] Caspi R, Altman T, Billington R, Dreher K, Foerster H, Fulcher CA, et al. The MetaCyc database of metabolic pathways and enzymes and the BioCyc collection of Pathway/Genome Databases. Nucleic Acids Res 2014;42:D459–71. https://doi.org/10.1093/nar/gkt1103.

[56] Lovell MA, Xie C, Markesbery WR. Decreased glutathione transferase activity in brain and ventricular fluid in Alzheimer's disease. Neurology 1998;51:1562–6. https://doi.org/10.1212/WNL.51.6.1562.

[57] Ryu W-I, Bormann MK, Shen M, Kim D, Forester B, Park Y, et al. Brain cells derived from Alzheimer's disease patients have multiple specific innate abnormalities in energy metabolism. Mol Psychiatry 2021;26:5702–14. https://doi.org/10.1038/s41380-021-01068-3.

[58] Weiss AKH, Loeffler JR, Liedl KR, Gstach H, Jansen-Dürr P. The fumarylacetoacetate hydrolase (FAH) superfamily of enzymes: multifunctional enzymes from microbes to mitochondria. Biochem Soc Trans 2018;46:295–309. https://doi.org/10.1042/BST20170518.

[59] SantaCruz KS, Yazlovitskaya E, Collins J, Johnson J, DeCarli C. Regional NAD(P)H:quinone oxidoreductase activity in Alzheimer's disease. Neurobiol Aging 2004;25:63–9. https://doi.org/10.1016/S0197-4580(03)00117-9.

[60] Saré RM, Cooke SK, Krych L, Zerfas PM, Cohen RM, Smith CB. Behavioral phenotype in the TgF344-AD rat model of Alzheimer's disease. Front Neurosci 2020: 14. https://doi.org/10.3389/fnins.2020.00601.

[61] Ameen-Ali KE, Easton A, Eacott MJ. Moving beyond standard procedures to assess spontaneous recognition memory. Neurosci Biobehav Rev 2015;53:37–51. https://doi.org/10.1016/j.neubiorev.2015.03.013.

[62] Da Rocha AS, Ferreira PCL, Bellaver B, Peixoto GGS, Venturin GT, Greggio S, et al. Longitudinal assessment of FDG-PET in the TgF344-AD rat. Alzheimers Dement 2021;17:e054136.

[63] Joo IL, Lai AY, Bazzigaluppi P, Koletar MM, Dorr A, Brown ME, et al. Early neurovascular dysfunction in a transgenic rat model of Alzheimer's disease. Sci Rep 2017;7:46427. https://doi.org/10.1038/srep46427.

[64] Akbari E, Asemi Z, Daneshvar Kakhaki R, Bahmani F, Kouchaki E, Tamtaji OR, et al. Effect of probiotic supplementation on cognitive function and metabolic status in Alzheimer's disease: A randomized, double-blind and controlled trial. Front Aging Neurosci 2016;8. https://doi.org/10.3389/fnagi.2016.00256.

[65] Vogt NM, Kerby RL, Dill-McFarland KA, Harding SJ, Merluzzi AP, Johnson SC, et al. Gut microbiome alterations in Alzheimer's disease. Sci Rep 2017;7:13537. https://doi.org/10.1038/s41598-017-13601-y.

[66] Zhuang Z-Q, Shen L-L, Li W-W, Fu X, Zeng F, Gui L, et al. Gut microbiota is altered in patients with Alzheimer's disease. J Alzheimers Dis 2018;63:1337–46. https://doi.org/10.3233/JAD-180176.

[67] Shin N-R, Whon TW, Bae J-W. Proteobacteria: microbial signature of dysbiosis in gut microbiota. Trends Biotechnol 2015;33:496–503. https://doi.org/10.1016/j.tibtech.2015.06.011.

[68] Scales BS, Dickson RP, Huffnagle GB. A tale of two sites: how inflammation can reshape the microbiomes of the gut and lungs. J Leukoc Biol 2016;100:943–50. https://doi.org/10.1189/jlb.3MR0316-106R.

[69] Long N, Deng J, Qiu M, Zhang Y, Wang Y, Guo W, et al. Inflammatory and pathological changes in Escherichia coli infected mice. Heliyon 2022;8:e12533. https://doi.org/10.1016/j.heliyon.2022.e12533.

[70] Lin CK, Kazmierczak BI. Inflammation: A double-edged sword in the response to pseudomonas aeruginosa infection. J Innate Immun 2017;9:250–61. https://doi.org/10.1159/000455857.

[71] Dandachi I, Anani H, Hadjadj L, Brahimi S, Lagier J-C, Daoud Z, et al. Genome analysis of Lachnoclostridium phocaeense isolated from a patient after kidney transplantation in Marseille. New Microbes New Infect 2021;41:100863. https://doi.org/10.1016/j.nmni.2021.100863.

[72] Folz J, Culver RN, Morales JM, Grembi J, Triadafilopoulos G, Relman DA, et al. Human metabolome variation along the upper intestinal tract. Nat Metab 2023: 1–12. https://doi.org/10.1038/s42255-023-00777-z.

[73] Gentreau M, Chuy V, Féart C, Samieri C, Ritchie K, Raymond M, et al. Refined carbohydrate-rich diet is associated with long-term risk of dementia and Alzheimer's disease in apolipoprotein E ε4 allele carriers. Alzheimers Dement 2020;16:1043–53. https://doi.org/10.1002/alz.12114.

[74] Meneilly GS, Hill A. Alterations in glucose metabolism in patients with Alzheimer's disease. J Am Geriatr Soc 1993;41:710–4. https://doi.org/10.1111/j.1532-5415.1993.tb07458.x.

[75] Southgate DA. Digestion and metabolism of sugars. Am J Clin Nutr 1995;62:203S-210S; discussion 211S. https://doi.org/10.1093/ajcn/62.1.203S.

[76] Yassine HN, Self W, Kerman BE, Santoni G, Navalpur Shanmugam N, Abdullah L, et al. Nutritional metabolism and cerebral bioenergetics in Alzheimer's disease and related dementias. Alzheimers Dement 2023;19:1041–66. https://doi.org/10.1002/alz.12845.

[77] Taylor MK, Sullivan DK, Swerdlow RH, Vidoni ED, Morris JK, Mahnken JD, et al. A high-glycemic diet is associated with cerebral amyloid burden in cognitively normal older adults. Am J Clin Nutr 2017;106:1463–70. https://doi.org/10.3945/ajcn.117.162263.

[78] Power SE, O'Connor EM, Ross RP, Stanton C, O'Toole PW, Fitzgerald GF, et al. Dietary glycaemic load associated with cognitive performance in elderly subjects. Eur J Nutr 2015;54:557–68. https://doi.org/10.1007/s00394-014-0737-5.

[79] Morrison DJ, Preston T. Formation of short chain fatty acids by the gut microbiota and their impact on human metabolism. Gut Microbes 2016;7:189–200. https://doi.org/10.1080/19490976.2015.1134082.

[80] Ozato N, Saito S, Yamaguchi T, Katashima M, Tokuda I, Sawada K, et al. Blautia genus associated with visceral fat accumulation in adults 20–76 years of age. npj Biofilms Microbiomes 2019;5:1–9. https://doi.org/10.1038/s41522-019-0101-x.

[81] Xu C, Zhu H, Qiu P. Aging progression of human gut microbiota. BMC Microbiol 2019;19:236. https://doi.org/10.1186/s12866-019-1616-2.

[82] Mergenthaler P, Lindauer U, Dienel GA, Meisel A. Sugar for the brain: the role of glucose in physiological and pathological brain function. Trends Neurosci 2013;36:587–97. https://doi.org/10.1016/j.tins.2013.07.001.

[83] Neth BJ, Craft S. Insulin resistance and Alzheimer's disease: bioenergetic linkages. Front Aging Neurosci 2017;9:345. https://doi.org/10.3389/fnagi.2017.00345.

[84] Tran TTT, Corsini S, Kellingray L, Hegarty C, Gall GL, Narbad A, et al. APOE genotype influences the gut microbiome structure and function in humans and mice: relevance for Alzheimer's disease pathophysiology. FASEB J 2019;33:8221–31. https://doi.org/10.1096/fj.201900071R.